

# Finite Difference Elastic Wave Modeling Including Surface Topography

Abdulaziz M. AlMuhaidib\*, Michael Fehler, M. Nafi Toksöz, and Yang Zhang, Earth Resources Laboratory, MIT

## SUMMARY

Surface topography and the weathered zone (i.e., heterogeneity near the earth's surface) have great effects on elastic wave propagation. Both surface waves and body waves are contaminated by scattering and conversion by the irregular surface topographic features. In this paper, we present a 2D numerical solver for the elastic wave equation that combines a 4<sup>th</sup>-order ADER scheme (Arbitrary high-order accuracy using DERivatives) with the characteristic variable method at the free surface boundary. The method is based on the velocity-stress formulation. We demonstrate the method by calculating synthetic seismograms for simple features.

## INTRODUCTION

Numerical modeling of the elastic wave equation plays a key role in almost every aspect of seismology as it provides a means of explaining the recorded signal associated with complex earth models. Most of the numerical schemes solving the wave equation are either based on the strong-formulation (e.g., finite difference and spectral methods) or the weak-formulation (e.g., finite elements and spectral finite elements).

Finite-element methods (weak-formulation) have an advantage over other numerical methods since they have the flexibility to model irregular boundary conditions. However, modeling seismic wave propagation with FE methods is (i) computationally much more expensive than finite difference especially in 3D, (ii) requires mesh generation and adaption which can be labor intensive and not easily automated and (iii) can impose stability restrictions due to the need for very small geometrical elements near the boundary and thus requiring very small time steps compared to finite-difference schemes.

The difficulties with finite difference modeling are mainly in representing and constructing the numerical grid near a topographic surface and in how to accurately satisfy the traction-free boundary conditions on the rough surface. Several approaches to handle irregular free surfaces in finite difference simulations exist in the literature, with different drawbacks. (i) The simplest approach is the heterogeneous formulation, also known as the vacuum method (Kelly et al., 1976; Virieux, 1986; Muire et al., 1992.) This implicit approach is implemented easily by setting the elastic parameters above the free surface to vanish and using a small density value in the first velocity layer above the free surface to avoid a division by zero. However, the vacuum method is inaccurate (Greaves, 1996), and the accuracy of the solution decreases dramatically when the angle between the boundary and the meshing increases (Bohlen and Saenger, 2006). (ii) A second approach is to handle the free surface explicitly using the image method in staggered schemes, which was first developed to deal with flat surfaces (Levander, 1998) and then extended to irregular

topography (Jih et al., 1988; Robertsson, 1996; Ohminato and Chouet, 1997). However, the image method suffers from the discretization error due to the staircase approximation of the surface topography, which may have an effect on the physical conversion and scattered waves. (iii) A third approach to handle the surface topography is to use conformal mapping and solve the elastic wave equation in curvilinear coordinates (Tessmer et al., 1992; Zhang and Chen, 2006; Appelo and Petersson, 2009). This approach, however, requires mesh generation and adaption, and it involves expanding the first order hyperbolic velocity-stress equations in curvilinear coordinates, which can be very expensive for large-scale problems.

To avoid most of these drawbacks, we developed a 2D finite-difference solver that combines a 4<sup>th</sup>-order ADER scheme (Schwartzkopff et al., 2005) with the characteristic variable (CV) method (Gottlieb et al., 1982; Bayliss, 1986; Giese, 2009) at the free surface boundary. We refer to this method as ADER-CV. To validate this method, we benchmarked the finite difference solver with the conformal mapping method (Zhang and Chen, 2006.)

## FORMULATION OF ELASTIC WAVE MODELING

We followed the formulation of the elastodynamic equations. For a 2D Cartesian system with a horizontal positive  $x$ -axis pointing to the right, and a positive vertical  $z$ -axis pointing down, the basic governing equations that describe elastic wave propagation (in the velocity-stress formulation) are the equations of motion (Virieux, 1986)

$$\begin{aligned}\rho \frac{\partial v_x}{\partial t} &= \frac{\partial \sigma_{xx}}{\partial x} + \frac{\partial \sigma_{xz}}{\partial z}, \\ \rho \frac{\partial v_z}{\partial t} &= \frac{\partial \sigma_{zx}}{\partial x} + \frac{\partial \sigma_{zz}}{\partial z},\end{aligned}\quad (1)$$

and the constitutive laws for an isotropic medium:

$$\begin{aligned}\frac{\partial \sigma_{xx}}{\partial t} &= (\lambda + 2\mu) \frac{\partial v_x}{\partial x} + \lambda \frac{\partial v_z}{\partial z}, \\ \frac{\partial \sigma_{zz}}{\partial t} &= (\lambda + 2\mu) \frac{\partial v_z}{\partial z} + \lambda \frac{\partial v_x}{\partial x}, \\ \frac{\partial \sigma_{xz}}{\partial t} &= \mu \left( \frac{\partial v_x}{\partial z} + \frac{\partial v_z}{\partial x} \right),\end{aligned}\quad (2)$$

where  $v_x$  and  $v_z$  are the velocity components,  $\sigma_{ij}$  are the stresses,  $\lambda$  and  $\mu$  are the Lamé parameters, and  $\rho$  is density.

## IMPLEMENTATION OF FREE SURFACE CONDITION WITH SURFACE TOPOGRAPHY

## Finite Difference Elastic Wave Modeling Including Topography

### Free Surface Condition in 1D (Flat)

The boundary conditions at the free surface are zero normal and shear stresses  $\sigma_{xz} = \sigma_{zz} = 0$ . The interior scheme requires the use of two nodes in every direction from the point being advanced as shown in Figure 1. The boundaries are taken into account explicitly by using ghost points for points beyond the free surface to impose the physical boundary condition. Thus, at each time step, all boundary fluxes are updated at points outside the computational domain using the characteristic variable method (Gottlieb et al., 1982; Bayliss et al., 1986). The variables  $v_x$ ,  $v_z$ , and  $\sigma_{xx}$  are calculated by mirroring based on the characteristic variables, which are defined as:

$$\tilde{U} = \begin{bmatrix} v_x^g \\ v_z^g \\ \sigma_{xx}^g \\ \sigma_{zz}^g \\ \sigma_{xz}^g \end{bmatrix} = \begin{bmatrix} v_x + \frac{\sigma_{xz}}{\sqrt{\rho\mu}} \\ v_z + \frac{\sigma_{zz}}{\sqrt{(\lambda+2\mu)\rho}} \\ \sigma_{xx} - \sigma_{zz} \frac{\lambda}{(\lambda+2\mu)} \\ 0 \\ 0 \end{bmatrix}, \quad (3)$$

where  $v_x^g$ ,  $v_z^g$ ,  $\sigma_{xx}^g$ ,  $\sigma_{zz}^g$ , and  $\sigma_{xz}^g$  are the ghost values outside the computational domain obtained by mirroring the fluxes from the interior domain. Combining the free surface boundary condition with the mirrored fluxes of the characteristic variables makes it possible to obtain all of the dependent variables.

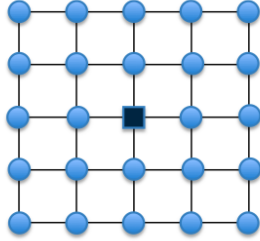


Figure 1: ADER 4<sup>th</sup> order stencil with 25 points.

### Free Surface Condition in 2D (Irregular)

The boundary treatment described in this section is based on the idea developed by (Forrer and Jeltch, 1998) for the Euler equations. The first step to find the mirror points inside the computational domain is to calculate the normal vector to the boundary for each ghost grid point. Therefore, we used the fast marching level set method (Sethian 1996) to compute the distance function of the free surface. Then, we used the distance function to find the mirror point inside the domain for each ghost point outside the domain as shown in Figure 2. The computation of the normal vector and the projection needs to be done only once, and its computational cost is negligible.

The mirror point is interpolated using a 2<sup>nd</sup> order accurate Lagrange interpolation method in two dimensions given by

$$P_j(x) = y_j \prod_{\substack{k=1 \\ k \neq j}}^n \frac{x - x_k}{x_j - x_k}.$$

where  $P(x)$  is the Lagrange interpolating polynomial of degree  $\leq (n - 1)$  that passes through the  $n$  points  $(x_1, y_1 = f(x_1))$ ,  $(x_2, y_2 = f(x_2))$ ,  $(x_n, y_n = f(x_n))$ . To estimate a point in two dimensions, the Lagrange interpolation is applied twice, once along each direction.

In order to mirror the fluxes of the characteristic variables, we rotated the coordinate frame by an angle  $\theta$ , so the normal direction is pointing in the positive  $z$ -direction (vertical) in the new coordinate frame; then we determine the ghost values before rotating back to the original coordinate frame. The idea can be summarized as follows:

- Transform the stresses and velocities into a local coordinate frame  $\tilde{U}_i = R_\theta U_i$
- Obtain the ghost state vector  $\tilde{U}_g$  using the characteristics as shown in (3)
- Rotate back to the original coordinate frame  $U_g = R_{(-\theta)} \tilde{U}_g$

where  $R_\theta$  is a linear transformation matrix.

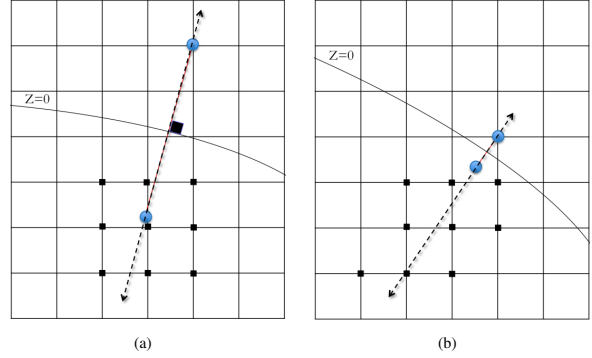


Figure 2: Determination of ghost values required for time-marching at neighboring grid nodes. The blue circles correspond to the ghost point (outside the domain) and its orthogonal projection on the surface (inside the domain). Lagrange interpolation (a) and extrapolation (b) in 2D are used to estimate the point inside the domain that will be then used to impose the boundary condition at the ghost point.

## NUMERICAL EXPERIMENTS

In order to validate the ADER-CV method, we consider both Gaussian and ramp shaped free surface models. We simulated the excitation of an explosive source by adding a known value to the stress for a point source with a 10 Hz Ricker wavelet. A 2D homogeneous earth consisting of a free surface over a half-space is used as an example. The domain has  $501 \times 501$  grid points with  $5m$  grid spacing, that is  $2500m$  extent along each axis. The benchmark test was calculated with a Courant number of  $\left(\frac{\Delta t V_p}{\Delta x} = 0.9\right)$ , which satisfies the stability condition. The medium properties are:  $V_p = 2500m/s$ ,  $V_s = 1200m/s$ , and  $\rho = 2000kg/m^3$ . The number of grid points per shortest S-wavelength is about 10.

## Finite Difference Elastic Wave Modeling Including Topography

The source was located at the middle of the computational domain at  $1000m$  depth with a Gaussian shaped hill free surface ( $200m$  height and  $200m$  width) as shown in Figure 3a. Comparisons of the recorded pressure from the ADER-CV method and the boundary conformal method (Zhang and Chen, 2006) are shown in Figure 3b. The agreement between the results calculated by the two methods is excellent. A snapshot of the wave-field ( $v_z$ -component) showing the scattering and multiple reflections caused by the irregular surface is shown in Figure 4.

### Ramp shape topography

Lastly, we show a homogeneous model with a ramp shape free surface, in which the topography has a significant impact on the seismic response. The slope of the ramp edge has a discontinuity, making it an extreme topographic model.

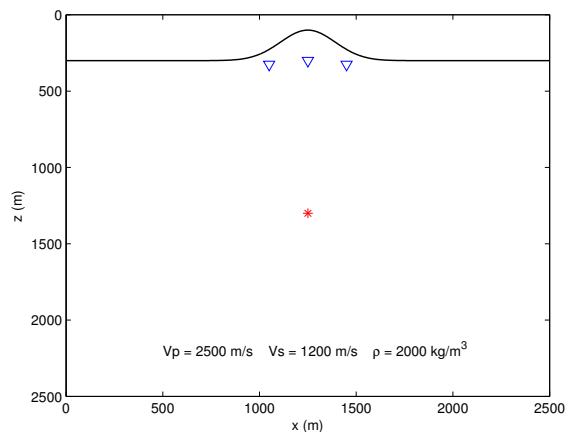
Time series of the velocity components along the free surface of the ramp shape model is shown in Figure 5. Due to the existence of sharp edges, strong and complex multiple body, shear and several Rayleigh wave packages are clearly identified on the synthetic seismograms. The method has also been applied to more complex models with surface topography and near surface heterogeneity.

## CONCLUSION

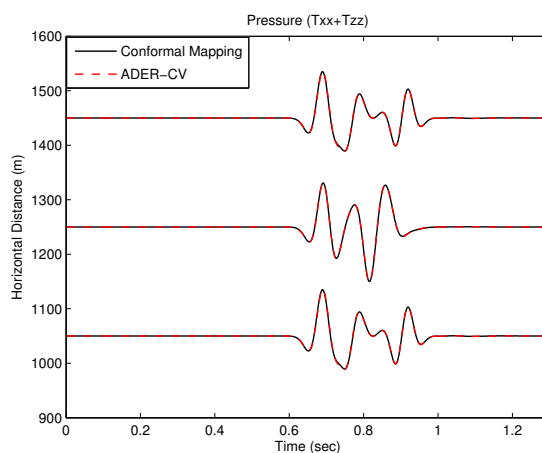
A 2D ADER time-domain single-grid finite difference approximation of first order PDEs that is  $4^{th}$  order accurate in time and space (with velocity-stress formulation) was developed to model wave propagation in linearly elastic and isotropic media with an irregular free surface. The characteristic variable method is implemented to account for the free surface B.C., and extended to handle arbitrary smooth boundaries. The scheme does not require mesh generation and adaption, and it does not involve expanding the governing equations in curvilinear coordinates, which can be computationally and labor intensive. The computational cost added by treating the topography is negligible compared to flat free surface as only a small number of grid points near the boundary needs to be computed.

## ACKNOWLEDGMENTS

We thank Wei Zhang for providing the benchmark results of the Gaussian-shape topography. We would like to thank Saudi Aramco and ERL founding members for supporting this research.



(a)



(b)

Figure 3: A Gaussian shaped hill. The computational domain is shown in (a): the source (red) and receivers (blue). (b) Comparisons of the recorded pressure at the receiver locations: ADER-CV (dashed-red) against the boundary conformal solution (black).

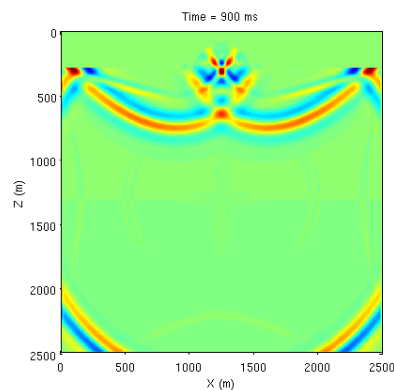
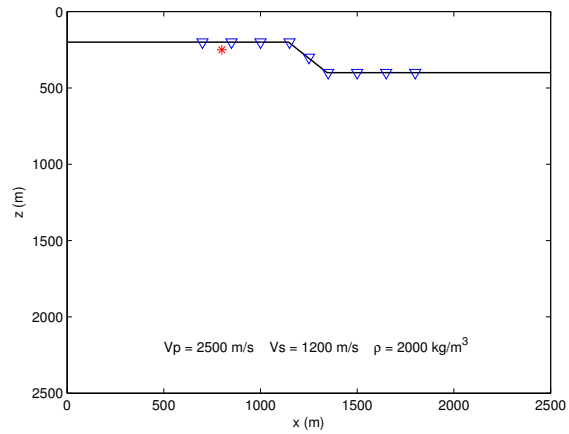
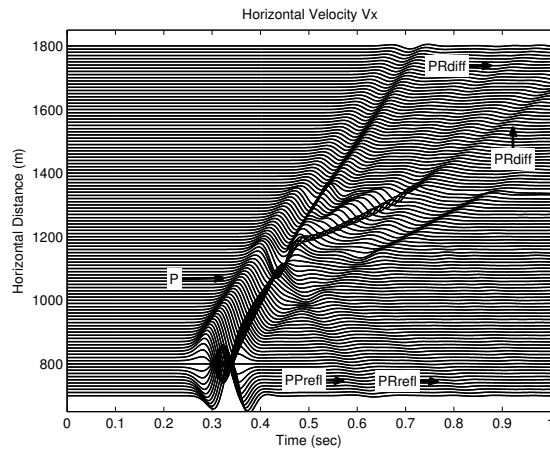


Figure 4: Snapshot of the wave-field  $v_z$  component showing the scattering and multiple reflections caused by the irregular surface shown in Figure 3a.

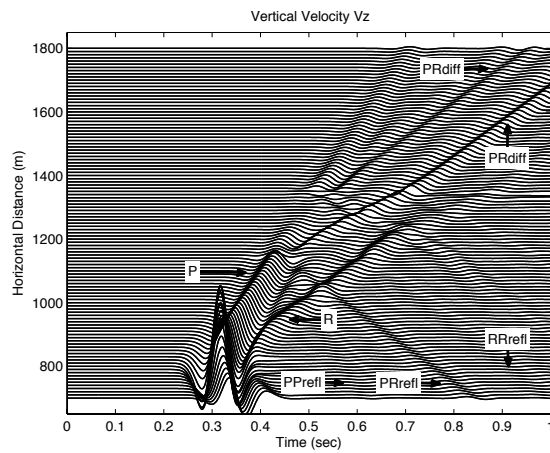
## Finite Difference Elastic Wave Modeling Including Topography



(a)



(b)



(c)

Figure 5: Time series of the velocity components along the free surface of the ramp shape surface model in (a), (b) the horizontal velocity  $v_x$  and (c) the vertical velocity  $v_z$ . The obvious phases are labeled, where P indicates P-wave, R indicates Rayleigh wave, and PRrefl indicates P to Rayleigh reflection.